Characterization of Supported Vanadium Oxide Species on Silica: A Periodic DFT Investigation

ARTICLE *in* THE JOURNAL OF PHYSICAL CHEMISTRY C · JUNE 2009

Impact Factor: 4.77 · DOI: 10.1021/jp902818m

4 AUTHORS:

Mazharul Mohammad Islam
University of Bonn
46 PUBLICATIONS **516** CITATIONS
SEE PROFILE

Dominique Costa
MINES ParisTech
94 PUBLICATIONS **1,763** CITATIONS
SEE PROFILE

M. Calatayud
Pierre and Marie Curie University - Paris 6
86 PUBLICATIONS **1,808** CITATIONS
SEE PROFILE

Frederik Tielens
Collège de France
93 PUBLICATIONS **1,329** CITATIONS
SEE PROFILE

Characterization of Supported Vanadium Oxide Species on Silica: A Periodic DFT Investigation

Mazharul M. Islam,[†] Dominique Costa,[†] Monica Calatayud,[‡,§] and Frederik Tielens*[,∥,⊥]

Laboratoire de Physico-Chimie des Surfaces, UMR 7045, Ecole Nationale Supérieure de Chimie de Paris, 11 rue Pierre et Marie Curie, F-75231 Paris Cedex, France, UPMC Univ Paris 06, UMR 7616, Laboratoire de Chimie Théorique, F-75005 Paris, France, CNRS, UMR 7616, Laboratoire de Chimie Théorique, F-75005 Paris, France, UPMC Univ Paris 06, UMR 7197, Laboratoire de Réactivité de Surface, Tour 54-55, 2ème étage - Casier 178, 4, Place Jussieu, F-75005 Paris, France, and CNRS, UMR 7197, Laboratoire de Réactivité de Surface, Tour 54-55, 2ème étage - Casier 178, 4, Place Jussieu, F-75005 Paris, France

Received: March 29, 2009; Revised Manuscript Received: May 4, 2009

The geometry, energetic, and spectroscopic properties of molecular structures of silica-supported vanadium oxide catalysts are studied using periodic density functional calculations. Isolated vanadia units deposed on amorphous silica are modeled at low coverage, 0.44 atoms nm^{-2}. The models are built following the grafting process through the reaction of a vanadium precursor with surface silanols: $OV(OH)_3 + (Si{-}OH)_n \rightarrow OV(OH)_{3-n}(O{-}Si)_n + nH_2O$ (with $n = 1{-}3$). The most stable grafted structures involve one vanadyl group together with n(V−O−Si) bonds. The predominance of the vanadate groups is analyzed as a function of hydration by means of atomistic thermodynamics. At dehydrated conditions, the trigrafted pyramidal $OV(O{-}Si)_3$ species are predominant, whereas partial hydration stabilizes digrafted $OV(OH)(O{-}Si)_2$ and monografted $OV(OH)_2(O{-}Si)$ species. The harmonic vibrational spectra for selected models are compared to recent experimental infrared and Raman data, for representative bands, and vibrational modes. Hydration effects are discussed in terms of thermodynamic stability and vibrational spectra. The results obtained in this study show that the pyramidal $OV(O{-}Si)_3$, digrafted $OV(OH)(O{-}Si)_2$, and monografted $OV(OH)_2(O{-}Si)$ models can exist at a support surface, a trend in agreement with recent experimental findings.

1. Introduction

Oxide supported metal oxide catalysts are of great interest because of their numerous applications in the chemical, petroleum, and environmental industries.[1] Among these, the supported vanadium oxide materials are widely used in various selective oxidation reactions such as the ethane and propane conversion[2,3] or the selective reduction of NO_x with ammonia.[4,5] These catalysts consist of an active vanadium oxide phase deposited on the surface of a high-surface area oxide support, such as SiO_2, Al_2O_3, TiO_2, and ZrO_2. A key step to fully understand the catalytic activity is the characterization of the vanadium oxide (VO_x) under reaction conditions and the way it is anchored to the surface of the support material. The role of the support also represents a particularly interesting topic since it is well-known that the choice of the support material influences the activity of vanadia catalysts by several orders of magnitude.[1,6,7]

Silica-supported catalysts have recently received attention for their application in the direct oxidation of methane to formaldehyde, being the subject of many experimental studies (see for instance refs 8−13 and references therein) as well as theoretical modeling.[14−19] The main factors affecting the performance of such catalysts are the dispersion of the active phase and the hydration extent, both of them having a strong impact in the molecular form of the vanadia units.[10,11,20] There is general agreement in the isolated nature of the vanadia (vanadate) units in dehydrated catalytically active silica samples. Tetrahedral coordination is observed for the vanadium site leading to a pyramidal arrangement OVO_3.[12,13] However, other molecular forms have been proposed in the literature in the last years in particular for hydrated samples. Thus, Keller et al.[10] have studied the effect of hydration on the molecular structure of silica-supported vanadium oxide catalysts with different VO_x loadings by combined IR, Raman, UV−vis, and EXAFS spectroscopic techniques. They concluded that both the pyramidal $OV(O{-}Si)_3$ and the monografted $OV(OH)_2(O{-}Si)$ models can exist on the support surface, their relative ratio depending on the hydration degree of the catalyst material. For the dehydrated surface, the presence of two types of monomeric species was highlighted corresponding to two types of V(V) cations: (a) with one V═O bond and three bridging V−O−Si linkages and (b) with one V═O bond, two bridging V−O−Si linkages and one V−OH group. Hydroxylation of the dehydrated VO_x/SiO_2 catalysts starts with the formation of V−O−H bonds which is characterized by a (V−)O−H stretching band around 3660 cm^{-1}. Launay et al.[11] reported the dynamic behavior of vanadium surface species on specially prepared amorphous silica. The molecular species show a strong reversible evolution between the hydrated state in ambient air and the dehydrated one. Raman and IR spectroscopies allowed the identification of hydroxylated monomeric species $OV(OH)(O{-}Si)_2$ even under dehydrated conditions.[11] The stability of VO_4 species bonded by one or two bonds to the support has been supported by spectroscopic measurements together with the presence of V−OH groups.[21] The uncertainties about specific spectral

* To whom correspondence should be addressed. E-mail: frederik.tielens@upmc.fr.
[†] Ecole Nationale Supérieure de Chimie de Paris.
[‡] UPMC Univ Paris 06, UMR 7616.
[§] CNRS, UMR 7616.
[∥] UPMC Univ Paris 06, UMR 7609.
[⊥] CNRS, UMR 7609.

10.1021/jp902818m CCC: $40.75
Published on Web 05/26/2009

assignments together with the different preparation methods may lead to confusion in establishing the nature of the surface species present on the catalysts.[18]

To confirm the models derived from spectroscopic data, quantum chemical ab initio calculations are required. An important obstacle to simulate the silica support is its amorphous structure. Amorphous silica exhibits a diversity of sites, especially in hydrous conditions: there are terminal and geminate silanols, and diversity in H bond connectivity. Moreover, a good model needs the presence of rings in order to account for the coupled movement of silicon atoms.[18] Some of us recently proposed a representative model for the hydroxylated amorphous silica surface[22] where the silanol density (5.8 OH/nm^2) and the geminate/terminal ratio (23% geminate) is that found on real samples, and accounts for the presence of different types of rings. This model will be used in the present work to explore the grafting of a vanadium precursor, O=V(OH)$_3$, to the silica surface.

In the present study, we perform a systematic theoretical investigation on the possible atomic models of the silica supported vanadium oxide catalysts in hydrated and dehydrated forms. The nature of the vanadate species is investigated from an inspection of the final geometry and corresponding total energy. Then, we use atomistic thermodynamics to bridge the gap between 0 K calculations and conditions of temperature and pressure used in the spectroscopic measurements. This allows us to estimate the predominance of the different species as a function of the temperature and hydration conditions. Finally, vibrational spectra are calculated and carefully compared with recent experimental results to assign representative bands.

2. Methodology

2.1. Computational Details. All calculations are performed using ab initio plane-wave pseudopotential approach as implemented in VASP.[23,24] The Perdew−Burke−Ernzerhof (PBE) functional[25,26] has been chosen to perform the periodic DFT calculations with an accuracy on the overall convergence tested elsewhere.[22,27−29] The valence electrons are treated explicitly and their interactions with the ionic cores are described by the projector augmented-wave method (PAW),[30,31] which allows to use a low energy cut off equal to 400 eV for the plane-wave basis. The gamma point is used in the Brillouin-zone integration. The positions of all the atoms in the super cell are relaxed until the total energy differences decrease below 10^{-4} eV.

Vibrational spectra have been calculated for selected surface species within the harmonic approximation. Only the vanadium center and its first neighbors (O−Si and OH groups) are allowed to move; the support is kept fixed. The Hessian matrix is computed by the finite difference method followed by a diagonalization procedure. The eigenvalues of the resulting matrix lead to the frequency values. The assignment of the vibrational modes is done by inspection of the corresponding eigenvectors.

2.2. Model Description. We start from the silica model structure described and characterized in our previous work[22] (Figure 1). The vanadium precursor is modeled by a VO(OH)$_3$ unit. This species is added to the silica unit cell (dimensions 12.77 × 17.64 × 25.17 Å^3) resulting in a vanadium coverage of 0.44 atoms nm^{-2}, close to the experimental preparations.[10,12,13] The VO(OH)$_3$ entity is grafted by dehydration to surface silanols, following the reaction:

$$\mathrm{OV(OH)_3} + (\mathrm{Si{-}OH})_n \rightarrow \mathrm{OV(OH)_{3-}}_n(\mathrm{O{-}Si})_n + n\mathrm{H_2O} \quad (n = 1{-}3) \quad (1)$$

Up to three silanols may be involved in the reaction yielding different modes of grafting: mono, di, and tri respectively n = 1−3 in eq 1. The oxidation state of vanadium in the models is always +5 and is not mentioned further in the text.

Several geometrical configurations are systematically investigated. Structures involving the different silanol types: isolated (Si−OH), vicinal (HO−Si−O−Si−OH), geminate (HO−Si−OH), and nonvicinal (two Si−OH groups not directly connected), on the surface were considered. Due to the flexibility of the silica surface, these species can be easily accommodated. The models are called V1, V2, and V3 corresponding to mono-, di-, and trigrafted structures (n = 1−3, respectively) with an additional letter if other grafting positions on the surface are considered. The reaction energy values ($\Delta E_{\mathrm{react}}$) of reaction (1) for several sites are compiled in Table 1. Figure 2 displays the structures retained for further discussion.

3. Results and Discussion

3.1. Geometry and Energetics. According to the calculated energy values for reaction (1) shown in Table 1, monografted species exhibit a preference for vicinal silanol sites followed by isolated and geminate silanol groups. This preference might be due to the formation of H-bonds between the vanadate V−OH groups and the surface silanol groups stabilizing certain conformations. Digrafted vanadate does not show any preference for vicinal or geminate groups. Note that the vanadate grafted to the vicinal sites forms a six-member ring (see Figure 2). Trigrafted species need the presence of three neighboring silanol sites and no preference for a particular configuration is found. Bridging hydroxyl groups V−OH-Si are clearly disfavored (not shown).

Figure 2 shows the most stable structures obtained after geometry optimization of V-grafted on one vicinal silanol (monografted V1-a), two vicinal silanols (digrafted V2-a with a common Si−O−Si linkage) and nonvicinal silanols (digrafted V2-b without a common Si−O−Si linkage), and three neighboring silanol groups (trigrafted V3). Table 2 shows selected geometrical parameters. The optimized structures are very similar, with a V=O bond of 1.60 Å, which is in agreement with the gas phase VO(OH)$_3$ molecule[5,32] and other calculated gas-phase clusters.[33] The vanadyl bond is not influenced by the

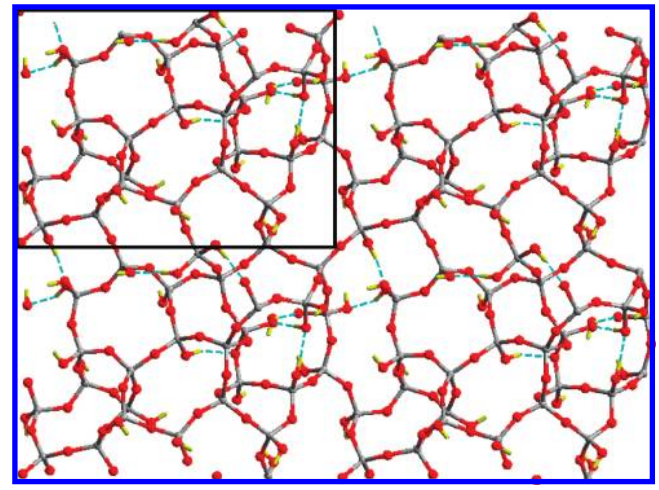

Figure 1. Model for the amorphous silica surface used in this work, showing the unit cell (dimensions 12.77 × 17.64 × 25.17 Å^3).

TABLE 1: Reaction Energy Calculated Using eq 1 for the Grafting of the Different Vanadium Oxide Species[a]

Structure	ΔE_{react}
V1-a (vicinal)[b]	−0.66
V1-b (geminate)	−0.30
V1-c (isolated)	−0.44
V2-a (vicinal)[b]	−0.25
V2-b (not vicinal)[b]	−0.24
V3[b]	+0.95

[a] Values in eV. [b] See Figure 2.

environment. The bridging V−OSi bond distances (1.63−1.65 Å) and the bond angle V−O−Si (around 160°) are also very similar, independent of the nature of the grafting site. The V−OH bonds are in the range 1.76−1.78 Å. The values obtained in the calculations are in nice agreement with atomic XAFS derived values reported in[21,34] (see Table 2): V═O (1.58 Å), V−OH (1.69 Å), V−OSi (1.80 Å). However, the V−Si value reported in those works (2.61 Å), is smaller than our calculated values (3.06−3.38 Å), and also the V−O−Si angle (101° in ref 21; ∼160° in this work). The reason for this disagreement might come from the model used (a VO_4 molecule without hydroxyl groups and a regular β-SiO_2(111) surface as support in ref 21; $OV(OH)_3$ molecule and amorphous hydroxylated silica in the present work) and the optimization procedure (Cerius[2], ref 33 in ref 21, periodic DFT in the present work).

The grafting of vanadium oxide on silica surface has a relative small effect on the silica framework. The largest distortion is observed for the bridging oxygen sites (V−O−Si). Initially silica hydroxyl groups, after grafting they are displaced 0.25 Å for the mono grafted, 0.50 Å for the di grafted and up to 1.3 Å for the tri grafted vanadium oxide. The next near neighbor Si atoms are slightly altered: they are displaced at most 0.3 Å from the initial positions in the trigrafted site; the mono- and di grafted systems do not exhibit significant distortion. The neighboring Si−O−Si angles within SiO cycles containing vanadium decrease at most 6°. The O−Si−O angles are less flexible and stay very close to the tetrahedral angle. In summary the overall silica geometry is only slightly modified upon V oxide grafting, the tri grafted site induces the largest distortion in the silica hydroxyl (silanol) anchoring points.

Depending on their density, surface silanols are generally interacting with their neighbors forming a H-bond network. The grafting reaction perturbs the local H-bond network in two ways: first, surface hydroxyl groups are removed upon grafting and second, the vanadate units might also form hydrogen bonds with the silica support. In the models studied, the V−OH groups bind to surface silanols with a stabilization of the structure. This is the case for models V1-a, V2-a, and V2-b. The formation of additional H-bonds coming from V−OH groups seems then to compensate for the loss of H-bonds between silanols after grafting.

To summarize, the nature of the silanol group (isolated, vicinal, and geminate) has no influence on the stability and geometry of the grafted precursor with the exception of the monografted species. The overall silica framework is only slightly modified upon V oxide grafting, the tri grafted site introduces the largest constrains. However, the silanol H-bond connectivity influences the overall reaction energy. The final result depends on the energetic balance of the number of H bonds broken/created.

Considering the reaction energy (ΔE_{react}, Table 1) as calculated according to reaction (1) for the best grafting modes (mono-, di-, and trigrafting), we obtain −0.66, −0.25, and +0.95 eV for $n = 1-3$, respectively. These values suggest that the adsorption of the vanadium complex is favored compared to the initial situation (hydroxylated silica and $O{=}V(OH)_3$ in the gas phase) for the mono- and digrafted species, while it is endothermic for the trigrafted one. The endothermicity of the reaction leading to the trigrafted species means that the gain in energy due to the formation of three water molecules is not enough to counter-balance the cost of breaking three Si−OH bonds. Indeed, the present calculations report electronic energies only, which are identical to the free energy at 0 K. Under a given temperature T and pressure p, the contributions of entropy and chemical potentials have to be taken into account in the free energies.

It is interesting to mention here that the synthesis of the grafted catalyst occurs experimentally through successive steps: after impregnation by the precursor at room temperature, in aqueous or non aqueous solution, the obtained surface is dried and then calcined to achieve a chemically grafted active site and to burn all reactive species still present at the surface. In the case of the V−SiO_2 synthesis, the samples are dried one night at room temperature or at 393 K, then calcined for several hours at 723−773 K, depending on the experimental works.[10,12,13] Thus, it is empirically known that a high temperature and dehydration conditions are necessary to obtain the pluri-grafted V-complex.

In order to get a more precise picture of the respective stabilities of the mono-, di-, and trigrafted species at the silica surface, we performed calculations using the atomistic thermodynamics approach. To take into account deviations in surface composition and the presence of gas phases, one introduces appropriate chemical potentials to calculate an approximation of the Gibbs free-surface energy. Assuming that the surface is in thermodynamic equilibrium with the gas phases, the chemical potentials are related to a given temperature T and pressure p. This procedure enables to extend the 0 K and zero pressure DFT results to experimentally relevant environments, thereby bridging the gap between ultrahigh vacuum like conditions, and temperatures and gas phase pressures that are applied in realistic catalytic conditions.

We will now consider the following equations:

$$OV(OH)_2(O-Si) \rightarrow OV(OH)(O-Si)_2 + H_2O(g) \quad (2)$$

$$OV(OH)(O-Si)_2 \rightarrow OV(O-Si)_3 + H_2O(g) \quad (3)$$

We consider that the vanadia/silica system is in contact with a gaseous water reservoir. From the electronic energy, the free energy of the water/vanadia/silica interface under known thermodynamic conditions may be estimated following the approximations used by Digne et al.,[35] as originating from Kaxiras et al.[36] and Qian et al.[37] It consists in the neglect of the variation of the chemical potentials of the surfaces with the adsorption and the consideration of the gas phase as a perfect gas. In the proposed scheme, the free energy of water (including the ZPE correction) in the gas phase is

$$\Delta G(H_2O) = E(H_2O) - ((\Delta H_G - T\Delta S_G(T)) + RT\ln(p/p^\circ)) \quad (4)$$

where $E(H_2O)$ is the electronic energy of water calculated at 0 K, ΔH_G and $\Delta S_G(T)$ are the enthalpy and entropy of gaseous water, calculated with the Gaussian 03 code[38] as a function of

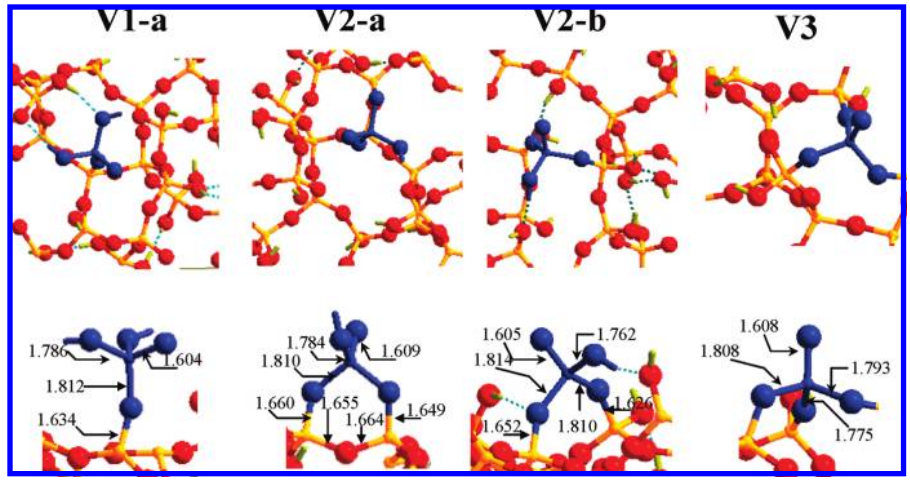

Figure 2. Most stable geometries for the supported $VO(OH)_3$ precursor, that is, mono- (1 V-a), di- (V2-a vicinal and V2-b not vicinal silanol groups), and trigrafted (V3) models. Distances in Å.

TABLE 2: Calculated and XAFS Derived Selected Geometrical Parameters in Vanadia/Silica Systems[a]

	this work	literature
d(V=O)	1.60−1.61	1.58[34]
d(V−OSi)	1.78−1.81	1.80[34]
d(VO−Si)	1.63−1.65	
d(V−OH)	1.76−1.78	1.69[34]
d(V−Si)	3.06[b]−3.38[a]	2.61[34]
α(V−O−Si)	158−164[a]	101[21]
	128−137[b]	
α(V−O−H)	118−124	

[a] Distances d in Å, angles α in degrees. [a] Monografted species. [b] Digrafted and trigrafted species.

the temperature, p is the partial pressure of water vapor, and $p°$ is the standard pressure (1 bar).

Using the above-mentioned formalism, the free energy of reactions (2) and (3) for the formation of the di- and trigrafted vanadium complexes from the monografted one at equilibrium conditions, are then expressed as

$$\Delta G_2 = E(\mathrm{OV(OH)(O{-}Si)_2}) + \Delta G(\mathrm{H_2O}) - E(\mathrm{OV(OH)_2(Si{-}O)})$$

$$\Delta G_3 = E(\mathrm{OV(O{-}Si)_3}) + \Delta G(\mathrm{H_2O}) - E(\mathrm{OV(OH)(Si{-}O)_2})$$

In this approach, we consider that the energies of the mono- to di- and di- to trigrafted transitions are independent of the degree of hydration of the silica surface. It is known experimentally that silanols are stable at silica surfaces until 673 K. Above this temperature, silanols begin to condensate into siloxane bridges.[39] Thus, our model with 5.8 OH/nm^2 corresponding to conditions of a hydroxylated surface, remains valid until the temperature of 673 K.

Figure 3 shows the surface free energy Γ, defined as the free energy per surface area, of the di- and trigrafted V-complexes on the silica surface as a function of temperature (T) for a water partial pressure (p) equivalent to the ambient air water partial pressure (p_w = 1500 Pa).[40] At these conditions, the monografted model is the most stable until T = 220 K, followed by the digrafted structure in the 220−550 K domain, finally at T > 550 K the trigrafted complex is found as the most stable configuration. These results are fully consistent with the experimental procedure used in the synthesis of vanadia-supported catalysts by grafting methods,[10,12,13] where samples are heated and annealed at high temperatures to obtain $O{=}VO_3$ surface structure. Note that such species correspond to completely dehydrated conditions. In hydrated conditions (high water pressure or low temperature) mono- and digrafted structures are successively stabilized.

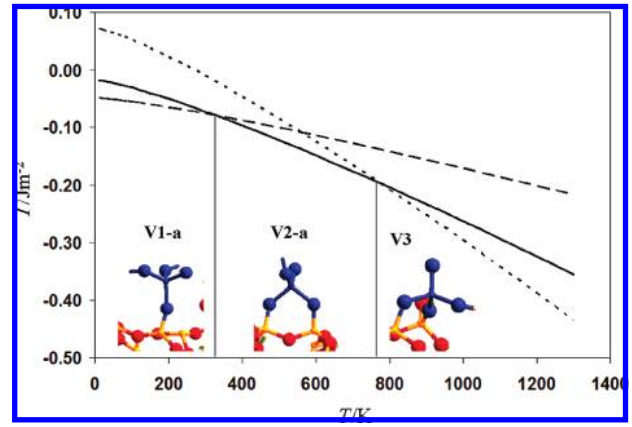

Figure 3. Phase diagram (surface energy vs temperature) showing the stability ranges for the different grafting geometries.

From the thermodynamic approach one concludes that the most stable species at low temperature is the monografted $OV(OH)_2(O{-}Si)$ complex. This configuration corresponds to the fully hydrated vanadia catalyst on the silica support, as suggested by Keller et al.[10] An increase in temperature or a decrease in hydration stabilizes the digrafted $OV(OH)(O{-}Si)_2$ complex as observed in ref 11. High temperatures favor the formation of the pyramidal $OV(O{-}Si)_3$ arrangement.[10−13]

In summary, the three grafted species may exist on a silica surface depending on the experimental conditions. In dehydrated conditions (high temperatures, low partial pressures) the pyramidal $OV(O{-}Si)_3$ is stabilized, while in hydrated conditions (low temperatures, high water pressures) the hydroxylated species $OV(OH)_2(O{-}Si)$ and $OV(OH)(O{-}Si)_2$ are predominant. They are supposed to reversibly interconvert in the presence of water, and they might coexist on the surface. This picture is fully consistent with recent works[10−13] and explains the different results found.

3.2. Vibrational Frequency Analysis. Table 3 shows the vibrations calculated for the models considered, together with the assignment of the normal modes. Only frequencies in the range 750−4000 cm^{-1} are reported. The typical feature of all

TABLE 3: Calculated Frequencies for Selected Models, in cm^{-1}[a]

model	frequency	mode	scaling factor	corrected
V1-a	3662	VO-H stretching (H bond 2.293 Å)	0.987	3616
	3567	VO-H (H bond 2.133 Å)	0.987	3522
	1062	V=O	0.978	1038
	961	V−O−Si stretching	0.942	905
	794	VO-H bending	0.987	784
	761	VO-H bending	0.987	752
V2-a	3752	V−OH (free)	0.987	3704
	1062	V=O	0.978	1039
	979	Si−O−Si asym stretching	1.000	979
	936	V−O−Si sym stretching	0.942	882
	829	V−O−Si asym stretching	0.942	781
	773	V−OH bending	0.942	728
V2-b	3267	VO-H stretching	0.987	3226
	1069	V=O	0.978	1045
	994	V−O−Si sym stretching	0.942	936
	916	V−O−Si asym stretching	0.942	863
	830	V−OH bending	0.987	820
	812	V−OH bending	0.987	802
V3	1054	V=O	0.978	1031
	986	V−O−Si sym stretching	0.942	929
	886	V−O−Si asym stretching	0.942	835
	856	V−O−Si asym stretching	0.942	807

[a] The scaling factor is derived from fitting selected vibrations to the experimental data reported in ref 10.

of the structures is the vibration at ∼1064 cm^{-1} associated to the vanadyl group stretch.

The region of 3000−4000 cm^{-1} is dominated by the hydroxyl vibrations. Values higher than 3660 cm^{-1} are assigned to free VO-H stretching modes (models V1-a and V2-b). Experimentally a narrow band is present at 3660 cm^{-1} upon hydroxylation of dehydrated samples which is assigned to the stretching of free VO-H groups.[10] Lower values indicate hydrogen bonding: 3567 cm^{-1} (V1-a, distance O...H=2.133 Å) and 3267 cm^{-1} (V2-b, distance O...H=1.720 Å).

The region between 1000 cm^{-1} and 800 cm^{-1} is dominated by V−O−Si stretching modes. There is dispersion in the values due to the different nature of the supported vanadia units. Thus, the monografted model V1-a shows a vibration at 961 cm^{-1}. The digrafted model V2-b shows V−O−Si vibrations at 936 cm^{-1} (symmetric), 829 cm^{-1} (asymmetric); the 979 cm^{-1} value corresponds to the Si−O−Si asymmetric stretch coupled to the O−V−O unit, in agreement with the observed IR band at 975 cm^{-1} assigned to silica support vibrations.[10] Note that in the V2-b model, a six member ring is formed involving O−V−O and Si−O−Si fragments, the latter corresponding initially to vicinal Si−OH groups. This ring is absent in model V2-a, since the silicon atoms involved are no longer vicinal. The calculated vibrations for V2-a present higher values: 994 cm^{-1} (symmetric) and 916 cm^{-1} (asymmetric). The trigrafted species V3 shows a symmetric stretching vibration at 986 cm^{-1}, and asymmetric stretch modes at 886 cm^{-1} and 856 cm^{-1}. Finally, the V−OH bending modes appear in the 750−830 cm^{-1} region overlapping with the lowest V−O−Si frequencies.

However, the calculated vibrations are overestimated with respect to the bands observed due to the use of DFT method and the harmonic approximation. In order to correct this feature a set of scaling factors have been derived based on a careful analysis of the recent IR and Raman measurements.[10] We have focused on the values reported for experimental sample 4 V−Si of Keller et al.,[10] whose density of 0.47 V nm^{-2} is close to our calculated 0.44 V nm^{-2}. The scaling factors and the fitted values are reported in Table 3; a correlation chart with the corrected values is displayed in Figure 4. The analysis is done as follows. For the hydrated catalyst, both IR and Raman spectra show a small peak at 3660 cm^{-1} assigned to (V-)O−H. Compared to our calculated value of free OH groups (models V1-a and V2-b), a scaling factor of 0.987 is derived. Applying this factor to the calculated vibrations for hydrogen bonded hydroxyl groups (V1-a, V2-a), shifts the values to lower frequencies between 3522 and 3226 cm^{-1}. These corrected values are fully consistent with the experimental observation made for hydrated catalysts:[10] the IR band broadens dramatically, the intensity increases and shifts to 3400 cm^{-1}. The vanadyl V=O band is observed at 1040 cm^{-1}[10-13] for which a scaling factor of 0.978 is derived.

The assignment of the bands in the 1000−800 cm^{-1} region is more complex, partly because of the different assignments done in the past (see discussion in[10]). Our investigation clearly indicates that this region corresponds to the V−O−Si vibrations confirming previous calculated data on similar systems.[18] Vibrational modes in this region should be IR active since they correspond to changes in the dipole moment perpendicular to the surface. A finer analysis of the results

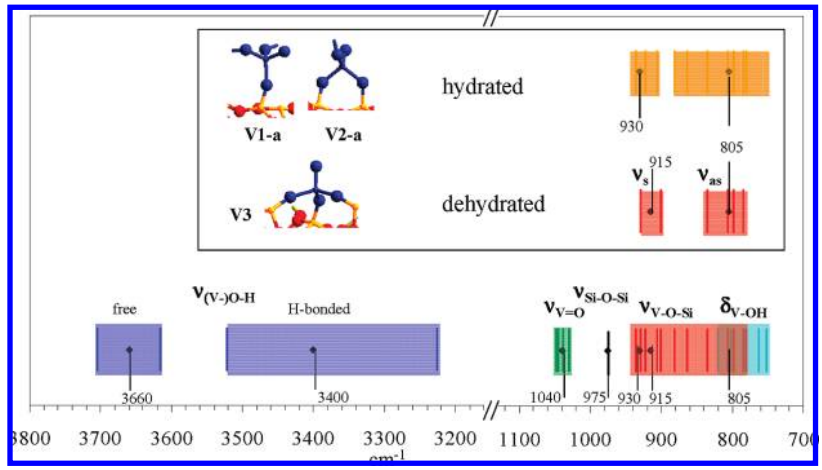

Figure 4. Correlation chart for the vibrations of isolated vanadia units supported on silica. The following correction factors have been used: 0.987 (OH), 0.978 (V=O), 0.942 (V−O−Si), and 1.000 (Si−O−Si) based on experimental values in ref[10] (see text and Table 2). The experimental values are displayed. Inset: bands are decomposed into hydrated and dehydrated contributions (see models in Figure 2).

(Table 3) leads to two sets of data corresponding to different hydration conditions: dehydrated model (V3) and hydrated models (V1-a, V2-a, and V-2b). Thus, the trigrafted species (V3) show a band around 970 cm^{-1} (uncorrected values), and a set of bands at 866 −833 cm^{-1}, assigned to symmetric and asymmetric stretching modes, respectively. These models represent dehydrated conditions and the calculated vibrations at 970 cm^{-1} can be compared to the experimental values of the dehydrated 4 V−Si sample in ref 10 at 915 cm^{-1}. A scaling factor of 0.942 is derived and applied to all the calculated V−O−Si frequencies. As can be seen in Figure 4, the dehydrated condition models lead to two groups of vibrations: a band around 915 cm^{-1} and a second one at around 800 cm^{-1}, in agreement with the IR bands (915 cm^{-1} and a broader band at 805 cm^{-1}) reported in.[10] The hydrated models show higher dispersion and slightly higher frequencies than the dehydrated ones, in agreement with the observed IR spectrum for hydrated samples (bands at 930 and 805 cm^{-1}). No clear distinction is observed between symmetric or asymmetric modes regions. The V−OH bending mode appears at lower frequencies and overlaps with the low V−O−Si vibrations. It has been corrected with the scaling factor of 0.987 derived for hydroxyl groups although the nature of the vibration is different. Our calculated spectra are fully consistent with the experimental observations.

Previous DFT calculations based on cluster models[18] lead to similar results for the dehydrated species. The V═O stretching mode is calculated to vibrate around 1045 cm^{-1}. The V−O−Si modes are split into an in-phase (symmetric) and out-of-phase (asymmetric) bands. The calculated intensity for the two V−O−Si bands in that work is similar; however, the former is calculated to vibrate at 1010 cm^{-1}, almost overlapping with the vanadyl stretching mode, whereas the latter is expected at 880 cm^{-1}. As the authors point out, the calculated frequencies show a stronger dependence on the model choice.

4. Conclusions

The molecular structures of oxide supported vanadia catalysts were determined theoretically by periodic quantum chemical calculations. Isolated vanadia units were deposed on the amorphous silica support at low coverage (0.44 atoms nm^{-2}) as found on commercial silica supports or mesoporous materials. Different models were built depending on the grafting site and hydration. It was found that the most stable structures involve one vanadyl group together with n(V−O−Si) bonds. The predominance of the vanadate groups was analyzed as a function of hydration by means of atomistic thermodynamics. It was observed that for the dehydration conditions, the trigrafted $OV(O-Si)_3$ species are predominant, whereas partial hydration stabilizes digrafted $OV(OH)(O-Si)_2$ and monografted $OV(OH)_2(O-Si)$ species. High temperature stabilizes the trigrafted structures whereas low temperatures favor the formation of partially hydrated digrafted and monografted species. Under certain conditions these species might coexist on the silica surface.

The calculated harmonic vibrational spectra for selected models were compared to recent experimental infrared and Raman measurements, with scaling factors and vibrational modes derived for representative bands: 3660 cm^{-1} (VO−H stretching), 1040 cm^{-1} (V═O), 915 cm^{-1} (V−O−Si symmetric stretching), 805 cm^{-1} (V−O−Si asymmetric stretching), 780 cm^{-1} (V−OH bending), bringing a clear interpretation of the experimental spectra.

The hydration effects in terms of thermodynamic stability and vibrational spectra of the various possible models are fully consistent with experimental data and permit to identify the molecular structure of the vanadium sites on the silica surface.

Acknowledgment. We gratefully thank T. Visser and B. Weckhuysen (Utrecht University, The Netherlands) for providing us with IR and Raman spectra. Computing facilities by CCRE, IDRIS, and CINES are acknowledged.

References and Notes

(1) Wachs, I. E. *Catal. Today* **2005**, *100*, 79.
(2) Bañares, M. A. *Catal. Today* **1999**, *51*, 319.
(3) Ballarini, N.; Cavani, F.; Cericola, A.; Cortelli, C.; Ferrari, M.; Trifiro, F.; Capannelli, G.; Comite, A.; Catani, R.; Cornaro, U. *Catal. Today* **2004**, *91−2*, 99.
(4) Busca, G.; Lietti, L.; Ramis, G.; Berti, F. *Appl. Catal. B* **1998**, *18*, 1.
(5) Calatayud, M.; Mguig, B.; Minot, C. *Surf. Sci. Rep.* **2004**, *55*, 169.
(6) Deo, G.; Wachs, I. E. *J. Catal.* **1994**, *146*, 323.
(7) Weckhuysen, B. M.; Keller, D. E. *Catal. Today* **2003**, *78*, 25.
(8) Berndt, H.; Martin, A.; Bruckner, A.; Schreier, E.; Muller, D.; Kosslick, H.; Wolf, G. U.; Lucke, B. *J. Catal.* **2000**, *191*, 384.
(9) Fornes, V.; Lopez, C.; Lopez, H. H.; Martinez, A. *Appl. Catal. A* **2003**, *249*, 345.
(10) Keller, D. E.; Visser, T.; Soulimani, F.; Koningsberger, D. C.; Weckhuysen, B. M. *Vibrat. Spectrosc.* **2007**, *43*, 140.
(11) Launay, H.; Loridant, S.; Pigamo, A.; Dubois, J. L.; Millet, J. M. M. *J. Catal.* **2007**, *246*, 390.
(12) Lee, E. L.; Wachs, I. E. *J. Phys. Chem. C* **2007**, *111*, 14410.
(13) Lee, E. L.; Wachs, I. E. *J. Phys. Chem. C* **2008**, *112*, 6487.
(14) Dobler, J.; Pritzsche, M.; Sauer, J. *J. Am. Chem. Soc.* **2005**, *127*, 10861.
(15) Ferreira, M. L.; Volpe, M. *J. Mol. Catal. A Chem.* **2002**, *184*, 349.
(16) Goodrow, A.; Bell, A. T. *J. Phys. Chem. C* **2007**, *111*, 14753.
(17) Khaliullin, R. Z.; Bell, A. T. *J. Phys Chem. B* **2002**, *106*, 7832.
(18) Magg, N.; Immaraporn, B.; Giorgi, J. B.; Schroeder, T.; Baumer, M.; Dobler, J.; Wu, Z. L.; Kondratenko, E.; Cherian, M.; Baerns, M.; Stair, P. C.; Sauer, J.; Freund, H. J. *J. Catal.* **2004**, *226*, 88.
(19) Rozanska, X.; Fortrie, R.; Sauer, J. *J. Phys. Chem. C* **2007**, *111*, 6041.
(20) Gao, X. T.; Bare, S. R.; Weckhuysen, B. M.; Wachs, I. E. *J. Phys. Chem. B* **1998**, *102*, 10842.
(21) Keller, D. E.; Koningsberger, D. C.; Weckhuysen, B. M. *J. Phys. Chem. B* **2006**, *110*, 14313.
(22) Tielens, F.; Gervais, C.; Lambert, J. F.; Mauri, F. C., D. *Chem. Mater.* **2008**, *20*, 3336.
(23) Kresse, G.; Hafner, J. *Phys. Rev. B* **1993**, *47*, 558.
(24) Kresse, G.; Hafner, J. *Phys. Rev. B* **1994**, *49*, 14251.
(25) Perdew, J. P.; Burke, K.; Ernzerhof, M. *Phys. Rev. Lett.* **1996**, *77*, 3865.
(26) Perdew, J. P.; Burke, K.; Ernzerhof, M. *Phys. Rev. Lett.* **1997**, *78*, 1396.
(27) Calatayud, M.; Tielens, F.; De Proft, F. *Chem. Phys. Lett.* **2008**, *456*, 59.
(28) de Bocarme, T. V.; Chau, T. D.; Tielens, F.; Andres, J.; Gaspard, P.; Wang, R. L. C.; Kreuzer, H. J.; Kruse, N. *J. Chem. Phys.* **2006**, 125.
(29) Tielens, F.; Andres, J. *J. Phys. Chem. C* **2007**, *111*, 10342.
(30) Blöchl, P. E. *Phys. Rev. B* **1994**, *50*, 17953.
(31) Kresse, G.; Joubert, D. *Phys. Rev. B* **1999**, *59*, 1758.
(32) Calatayud, M.; Mguig, B.; Minot, C. *Theor. Chem. Acc.* **2005**, *114*, 29.
(33) Calatayud, M.; Beltran, A.; Andrés, J. *J. Phys. Chem. A* **2001**, *105*, 9760.
(34) Keller, D. E.; Airaksinen, S. M. K.; Krause, A. O.; Weckhuysen, B. M.; Koningsberger, D. C. *J. Am. Chem. Soc.* **2007**, *129*, 3189.
(35) Digne, M.; Sautet, P.; Raybaud, P.; Euzen, P.; Toulhoat, H. *J. Catal.* **2002**, *211*, 1.
(36) Kaxiras, E.; Baryam, Y.; Joannopoulos, J. D.; Pandey, K. C. *Phys. Rev. B* **1987**, *35*, 9625.
(37) Qian, G. X.; Martin, R. M.; Chadi, D. J. *Phys. Rev. B* **1988**, *38*, 7649.
(38) Frisch, M. J.; Trucks, G. W.; Schlegel, H. B.; Scuseria, G. E.; Robb, M. A.; Cheeseman, J. R.; Vreven, T.; Kudin, K. N.; Burant, J. C.; Millam, J. M.; Iyengar, S. S.; Tomasi, J.; Barone, V.; Mennucci, B.; Cossi, M.; Scalmani, G.; Rega, N.; Petersson, G. A.; Nakasuji, H.; Hada, M.; Ehara, M.; Toyota, K.; Fukuda, R.; Hasegawa, J.; Ishida, M.; Nakajima, T.; Honda, Y.; Kitao, O.; Nakai, H.; Klene, M.; Li, X.; Knox, J. E.; Hratchian, H. P.; Cross, J. B.; Adamo, C.; Jaramillo, J.; Gomperts, R.; Stratmann, R. E.; Yazyev, O.; Austin, A. J.; Cammi, R.; Pomelli, C.; Ochterski, J. W.; Ayala, P. Y.; Morokuma, K.; Voth, G. A.; Salvador, P.; Dannenberg, J. J.; Zakrzewski, V. G.; SDapprich, S.; Daniels, A. D.; Strain, M. C.; Farkas,

O.; Malick, D. K.; Rabuck, A. D.; Raghavachari, K.; Foresman, J. B.; Ortiz, J. V.; Cui, Q.; Baboul, A. G.; Clifford, S.; Cioslowski, J.; Stefanov, B. B.; Liu, G.; Liashenko, A.; Piskorz, P.; Komaromi, I.; Martin, J. A.; Fox, D. J.; Keith, T.; Al-Laham, M. A.; Peng, C. Y.; Nanayakkara, A.; Challacombe, M.; Gill, P. M. W.; Johnson, B. G.; Chen, W.; Wong, M. W.; Gonzalez, C.; Pople, J. A. *Gaussian 03*, revision A.1; Gaussian, Inc.: Pittsburgh, PA, 2003.

(39) Bolis, V.; Fubini, B.; Marchese, L.; Martra, G.; Costa, D. *J. Chem. Soc. Faraday Trans.* **1991**, *87*, 497.

(40) Guyot, A.; Curtis, G. E.; Libbey, W. *Smithsonian Meteorological Tables: Based on Guyot's Meteorological and Physical Tables*; Smithsonian Institute: Washington, DC, 1896.

JP902818M